CHEMISTRY
A EUROPEAN JOURNAL

FULL PAPER

DOI: 10.1002/chem.200((will be filled in by the editorial staff))

The Synthesis of Functionalized Diaryltetraynes and their Transport Properties in Single-Molecule Junctions

Murat Gulcur,[a] Pavel Moreno-García,[b] Xiaotao Zhao,[a] Masoud Baghernejad,[b] Andrei S. Batsanov,[a] Wenjing Hong [b], Martin R. Bryce*,[a] and Thomas Wandlowski*,[b]

[a] Dr. M. Gulcur, X. Zhao, Dr. A. S. Batsanov, Prof. M. R. Bryce
Department of Chemistry, Durham University, Durham DH1 3LE (UK)
E-mail: m.r.bryce@durham.ac.uk

[b] Dr. P. Moreno-Garcia, M. Baghernejad, Dr. W. Hong, Prof. T. Wandlowski
Department of Chemistry and Biochemistry, University of Bern, Freiestrasse 3, CH-3012 Bern (Switzerland)
E-mail: thomas.wandlowski@dcb.unibe.ch

Keywords: Oligoynes / polyynes / cross-coupling / X-ray diffraction / single-molecule conductance / STM / MCBJ

Abstract. The synthesis and characterisation is described of six diaryltetrayne derivatives [Ar-(C≡C)$_4$-Ar] with Ar = 4-NO$_2$-C$_6$H$_4$- (**NO$_2$4**), 4-NH(Me)C$_6$H$_4$- (**NHMe4**), 4-NMe$_2$C$_6$H$_4$- (**NMe$_2$4**), 4-NH$_2$-(2,6-dimethyl)C$_6$H$_4$- (**DMeNH$_2$4**), 5-indolyl (**IN4**) and 5-benzothienyl (**BTh4**). X-ray molecular structures are reported for **NO$_2$4**, **NHMe4**, **DMeNH$_2$4**, **IN4** and **BTh4**. The stability of the tetraynes has been assessed under ambient laboratory conditions (20 ^{o}C, daylight and in air): **NO$_2$4** and **BTh4** are stable for at least six months without observable decomposition, whereas **NHMe4**, **NMe$_2$4**, **DMeNH$_2$4** and **IN4** decompose within a few hours or days. The derivative **DMeNH$_2$4**, with *ortho*-methyl groups partially shielding the tetrayne backbone, is considerably more stable than the parent compound with Ar = 4-NH$_2$C$_6$H$_4$ (**NH$_2$4**). The ability of the stable tetraynes to anchor in Au | molecule | Au junctions is reported. Scanning-tunneling-microscopy break junction (STM-BJ) and mechanically-controllable break junction (MCBJ) techniques are employed to investigate single-molecule conductance characteristics.

Introduction

The study of carbon-rich compounds is a very active research topic in organic synthesis and materials chemistry.[1,2] For example, sp^2 hybridized systems (e.g. graphene, nanotubes, fullerenes) are widely investigated due to their fascinating reactivity and their outstanding electronic and optical properties.[3] However, the *sp* hybridized carbon allotrope $(–C\equiv C)_\infty$ named carbyne is one of the least studied carbon allotropes due to its inaccessibility by standard synthetic routes and its insolubility.[4] Shorter chains of multiple conjugated alkyne units (i.e. diynes, oligoynes and polyynes) which possess terminal substituents to enhance their solubility and stability have been studied for many years.[5] They are fundamentally important molecules for experimental[6,7,8,9] and theoretical studies[10,11] of conjugation and charge-transport through carbon-rich backbones.

Oligoynes/polyyne chains $(–C\equiv C)_n$ have very attractive electron transport properties due to their almost cylindrical conjugation over the alternating single and triple bonds of the one-dimensional *sp*-backbone, leading to proposed applications as molecular wires, switches and non-linear optical components.[12,13] Theoretical studies suggest that polyynes could show metallic-like charge-transport characteristics when connected between two electrodes.[14,15]

The synthesis of oligoynes encounters problems as the stability decreases rapidly with the increasing number of the triple bonds in the backbone.[16] While a few C_8 derivatives [ie. $Ar–(C\equiv C)_4–Ar$, diaryltetraynes] and longer analogs with simple aryl end-groups are isolable at room temperature,[17] the established strategies for stabilizing derivatives with $n \geq 4$ alkyne units are: (i) to covalently attach very bulky aryl or organometallic end-groups,[18,19,20,21] (ii) to shield the oligoyne backbone within a supramolecular rotaxane-like structure,[22,23,24,25] or (iii) to encapsulate the polyyne within a carbon nanotube.[26] The vast majority of synthetic studies on oligo/polyynes have concerned ways to stabilize longer derivatives.[27] In contrast, little attention has been given to the synthesis of derivatives which might be suitable for molecular electronics applications. This requires functionalization with terminal substituents which will anchor the molecules to gold or other electrode materials.[28] The very bulky terminal groups which stabilize longer oligo/polyynes are not suitable for this purpose, and the traditional anchoring groups (e.g, amine, thiol) are expected to make oligoynes unstable in ambient conditions due to inter- or intra-molecular reactions of the anchor group with the oligoyne backbone, thereby cross-linking or degrading the molecules.[29]

In this context we have recently reported that diaryltetrayne derivatives (**Ar4**) (Chart 1) with terminal pyridyl (**PY**)[30] 4-cyanophenyl (**CN**) and 2,3-dihydrobenzo[*b*]thien-5-yl (**BT**) end groups can be isolated, purified and fully characterized under standard laboratory conditions (20 ^oC, daylight and in air).[31] The transport properties of the **PY4**, **CN4** and **BT4** derivatives in Au | single-molecule | Au junctions were studied by scanning tunneling microscopy (STM) and mechanically controllable break junction (MCBJ) methods.[31] However, the **Ar4** analogues with 4-aminophenyl (**NH_2**) and 4-

(thioacetyl)phenyl (**SAc**) end-groups rapidly decompose on attempted isolation and could not be purified.[31]

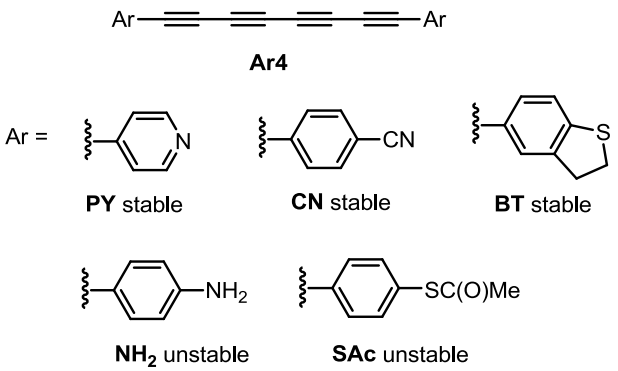

Chart 1. Structures of diaryltetraynes with functional end groups (ref. 31). For definitions of 'stable' and 'unstable' see text.

There is a need to explore new oligoynes to establish the scope of functionalized non-bulky end-groups which can be attached to the oligoyne chain and afford stable derivatives. We now present the synthesis of new diaryltetraynes with emphasis on derivatives which are stable under ambient conditions. Several new **Ar4** derivatives are characterized by spectroscopic methods and X-ray crystallography; the ability of the stable derivatives to anchor in molecular junctions is assessed and the electronic properties of Au | single-molecule | Au junctions are reported. This work provides the most comprehensive study to date on the synthesis of functionalized oligoynes and their applications in molecular junctions.

Results and Discussion

Synthesis

Diaryltetrayne compounds **Ar4a-f** were synthesized by dimerization of the trimethylsilyl protected precursor aryldiyne derivative **3a-f** under classical Eglington-Galbraith coupling conditions.[32] Compounds **3a-d**,**f** were synthesized by reaction of the corresponding aryliodide with 1,3-butadiyne-1-trimethylsilane. Due to the instability of 1,3-butadiyne-1-trimethylsilane (**2**) at high temperatures, compound **3e** was synthesized by a different route using 5-alkynylbenzo[*b*]thiophene **4** and trimethylsilyl acetylene. All steps proceeded in synthetically viable yields to afford the target diaryltetraynes **Ar4**. During the course of our work a similar synthesis of the nitrophenyl end-capped tetrayne **$NO_2$4** was reported by Szafert et al.[33]

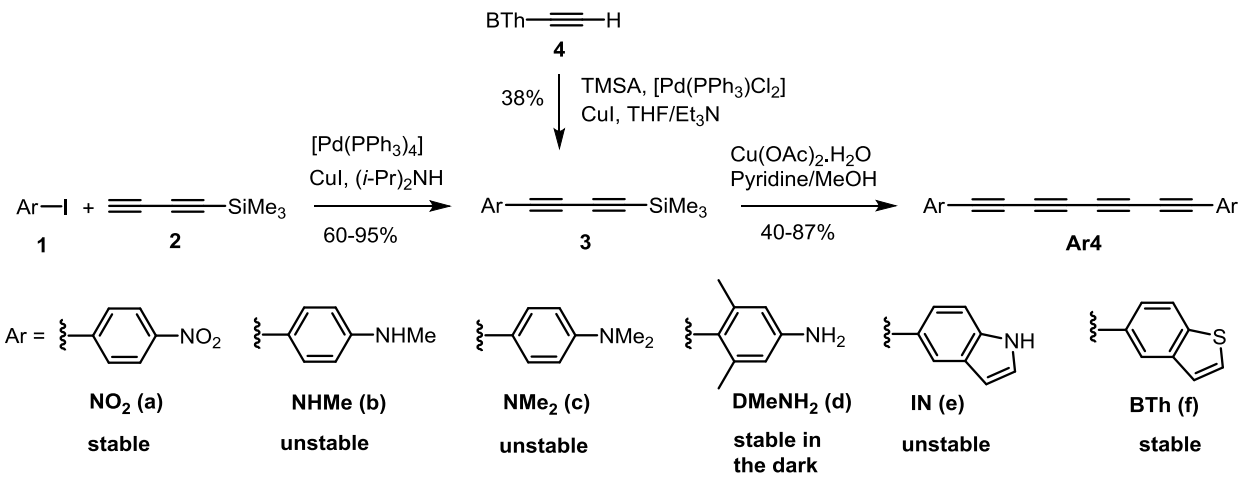

Scheme 1. Synthesis of diaryltetraynes **Ar4(a-f)**

Stability of the Diaryltetraynes

We will now discuss the stability of the tetrayne series. **$NO_2$4** is stable under ambient laboratory conditions and a solid sample can be stored for several months on the shelf with no observable decomposition. The compound has very low solubility and we could not characterize it by conventional solution NMR techniques. However, a high resolution mass spectrum and the X-ray crystal structure confirm the assigned structure.

In a previous study, the rapid decomposition under ambient conditions of 4-aminophenyl end-capped tetrayne **$NH_2$4** (Chart 1) was reported.[31] The probable decomposition process is an intermolecular reaction of the amino group with the *sp*-chain to form the observed dark-coloured insoluble product. In order to reduce the reactivity of the amine moiety, the mono- and di-methylated analogues **NHMe4** and **$NMe_2$4** were synthesized. In comparison to **$NH_2$4**, increased stability was observed for *N*-methylaniline end-capped tetrayne **NHMe4** which was characterized as soon as possible after isolation by ^{1}H, ^{13}C NMR, and mass spectroscopy. Crystals of **NHMe4** were grown in the dark. However, traces of decomposition products were seen and only limited stability under ambient conditions was observed for **NHMe4**. The dimethylamino analogue **$NMe_2$4** was found to be very light sensitive and attempts to grow crystals of **$NMe_2$4** were unsuccessful. During the preparation of this manuscript, the synthesis and X-ray crystal structure of the pentayne analogue terminated with bulkier 4-(diisopropylamino)phenyl groups was reported.[34]

Partially shielding the oligoyne chain by *ortho*-methyl groups, compound **$DMeNH_2$4**, considerably increased the stability compared to the parent compound **$NH_2$4**. **$DMeNH_2$4** was unambiguously characterized by ^{1}H and ^{13}C NMR spectroscopy, mass spectrometry and X-ray crystallography, using single crystals which were grown in the dark. The NMR spectra of **$DMeNH_2$4** provided no evidence

for decomposition upon storage in $CDCl_3$ in the NMR tube for 6 days in the dark after isolation. No precipitation or colour change of the solution was observed during this time. This sample was then exposed to ambient laboratory light; after 2 h the formation of an insoluble brown-black precipitate was observed.

5-Indolyl end–capped tetrayne **IN4** was also light sensitive and thermally unstable. It was characterized by ^{1}H and ^{13}C NMR and mass spectrometry immediately after purification. The instability was observed as a colour change of the bright yellow crystals to dark green when exposed to ambient light at room temperature. Crystals of **IN4** for X-ray analysis were grown in the dark. In contrast, the 5-benzothienyl analogue **BTh4** is stable for at least six months under ambient conditions.

To enable a comprehensive study to be undertaken of the length dependence of the single-molecule conductance for the NO_2 and BTh oligoyne series (see below), the corresponding butadiyne and tolane analogues were also synthesized (see Supporting Information).

X-Ray Crystal Structures of $NO_2$4, **NHMe4**, **$DMeNH_2$4, IN4 and BTh4**.

Molecules of **$NO_2$4**, **$DMeNH_2$4** (crystallized as acetone disolvate), **BTh4** and **IN4** have crystallographic C_i symmetry and therefore parallel arene rings. **NHMe4** has no crystallographic symmetry and its arene rings form a dihedral angle of 43° (Figure 1). The tetrayne rods in **$NO_2$4, $DMeNH_2$4** and **IN4** are practically linear, in the other two compounds they are substantially bent. In **NHMe4** the C(4)–C(7) and C(14)–C(15) bonds form an angle of 161.4°; in **BTh4** the central bond C(12)–C(12') forms 170.7° angles with C(7)–C(9) and C(7')–C(9') bonds. The molecular lengths are: **$NO_2$4** O(1)...O(1') 21.4; **NHMe4** N(1)...N(2) 20.0; **$DMeNH_2$4** N...N' 20.1; **IN4** N...N' 20.0 and **BTh4** S...S' 20.7 Å.

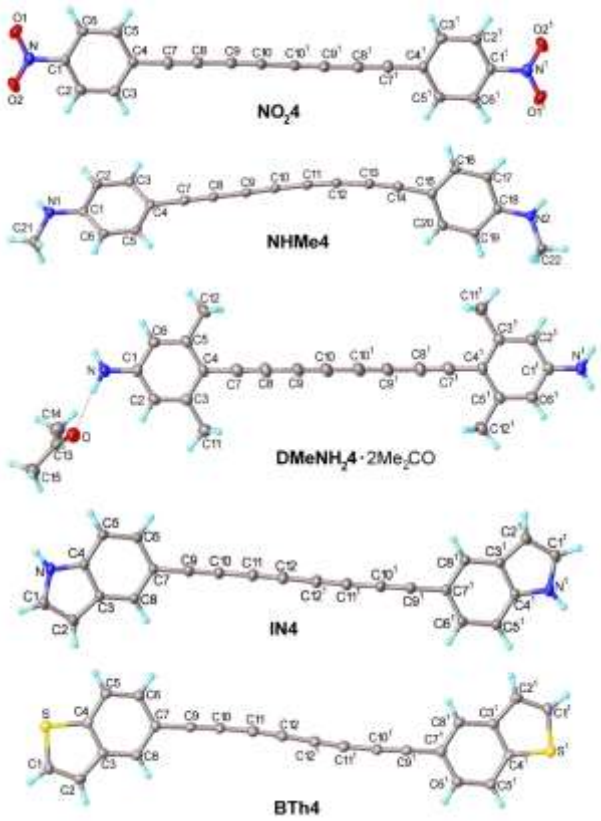

Figure 1. X-ray molecular structures of **$NO_2$4**, **NHMe4**, **$DMeNH_2$4, IN4** and **BTh4** showing thermal ellipsoids of 50% probability. Primed atoms are generated by inversion centres.

All five crystal structures comprise arrays of rigorously parallel, albeit offset, molecules related by a crystal lattice translation *a* (in **$NO_2$4**) or *b* (in all other cases). For **NHMe4** and **$DMeNH_2$4**, adjacent molecules in an array are linked by hydrogen bond bridges N-H···N-H···N and N-H···O···H-N-H···O···H-N, respectively. In **IN4**, weak N-H···N-H···N hydrogen bonds are zip together two adjacent arrays. In **$NO_2$4**, **NHMe4, BTh4** and **IN4** the shortest C···C distances between tetrayne rods (*d*) are close to the normal van der Waals contact (3.5 Å) and the arene end-groups are stacked in a π-π fashion (see Table 1). However, the slanting angle ϕ is not favourable for topotactic 1,8-polymerisation, for which d = 3.5 Å and ϕ = 21° are optimal.[33] The molecules of **$DMeNH_2$4** are intercalated by acetone of crystallisation, resulting in longer *d* and the absence of any effective overlap of the arene rings. Packing diagrams are shown in the Supporting Information.

Table 1. Crystal packing parameters

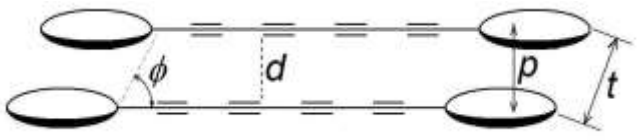

	ϕ (°)	t (Å)	d (Å)	p (Å)
$NO_2$4	78	3.74	3.68 – 3.69	3.38
NHMe4	66	3.99	3.62 – 3.69	3.41, 3.43
DMe$NH_2$4	58	5.23	4.42 – 4.51	--
IN4	50	4.86	3.78 – 3.84	3.31
BTh4	70	3.86	3.62 – 3.64	3.51

Single-Molecule Conductance Measurements

The transport properties of single oligoyne wires were studied by STM-BJ[35,36] and complementary MCBJ[37,38,39] measurements in solution at room temperature and in the absence of oxygen. The STM-BJ approach is based on the repeated formation and breaking of (single) molecule junctions formed between an atomically-sharp gold STM tip and a flat Au(111) substrate, and the simultaneous monitoring of the current i_T or conductance $G = i_T/V_{bias}$ in function of distance Δz at constant bias voltage V_{bias}. The MCBJ technique relies on the formation and rupture of molecular junctions between horizontally suspended gold wires.[37] For further technical details we refer to the Experimental Section and to our previous work.[38,39,40,41]

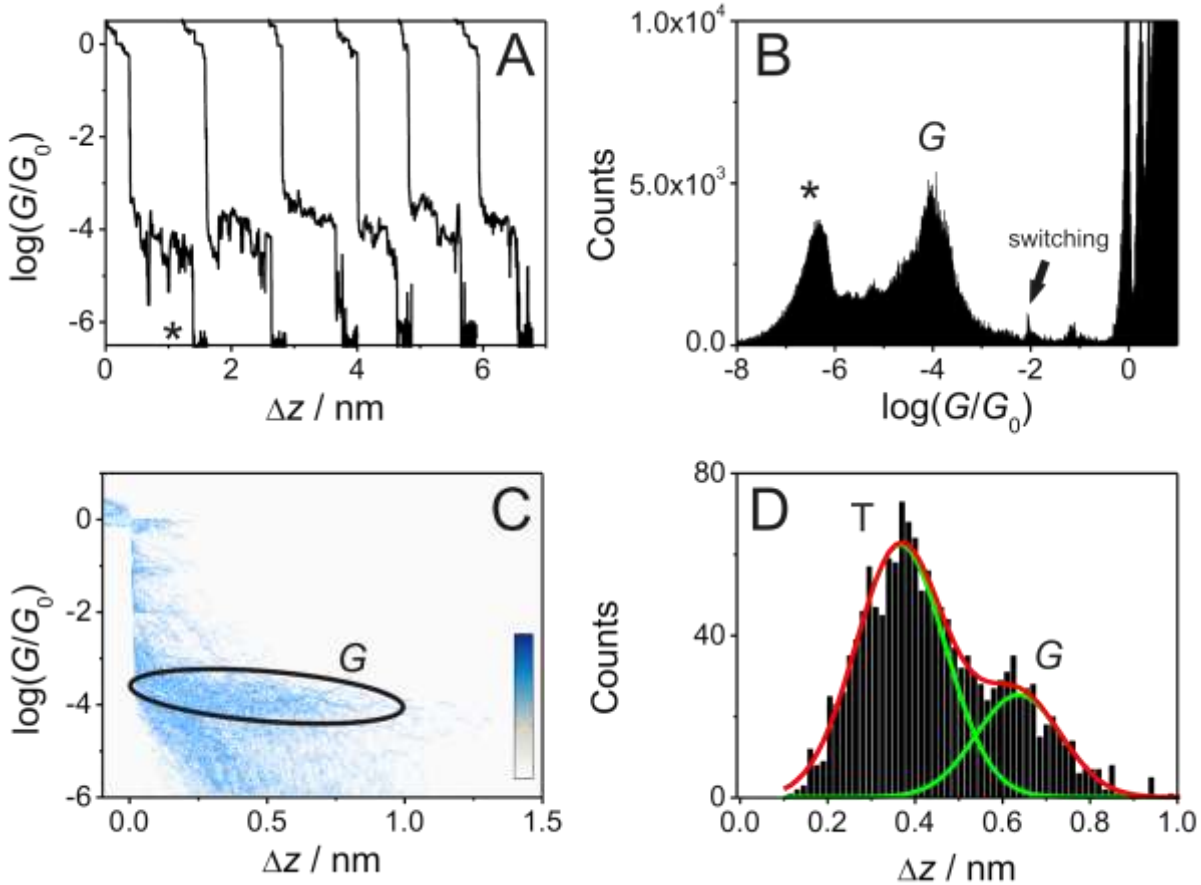

Figure 2. STM-BJ-based conductance measurements of **BTh4** in TMB/THF (5 : 1, v/v) as recorded with V_{bias} = 0.065 V and a stretching rate of 58 nm s^{-1}. (A) Typical original conductance vs. distance traces. (B) 1D conductance histogram. The noise level is indicated by the asterix. The small spike at log (G/G_0) ≈ -2 represents an artefact related to the switching of the amplifier. (C) 2D conductance histogram generated from 1600 individual curves without any data selection. (D) Characteristic relative displacement length histogram.[38]

Figure 2A displays, as an example, typical conductance (G) versus relative distance (Δz) stretching traces, plotted in a semi-logarithmic scale, as recorded for **BTh4** in TMB/THF. After formation of the contact between the gold tip and the Au(111) substrate, the tip was withdrawn with a rate of 58 nm s^{-1}. All curves show initially a step-like decrease of the conductance from 10 G_0 up to 1 G_0 with $G_0 = 2e^2/h$ = 77.5 μS being the quantum of conductance.[36] Subsequently, the conductance decreases abruptly by several orders in magnitude ("jump out of contact").[42] The very end of the gold contacts retract by approximately (0.5 ± 0.1) nm, the so-called snap-back distance Δz_{corr} (see refs. [31] and [38] for details). Additional features, such as plateaus are observed at $G \leq 10^{-3} G_0$, which are attributed to the formation of (single) molecular junctions. The noise level is reached at $G < 10^{-6}$ G_0 in the STM-BJ experiments.

Several thousands of individual G versus Δz traces were recorded and subsequently analyzed further by constructing all-data point histograms (without any data selection) to extract statistically significant results. Figure 2B displays the corresponding one-dimensional (1D) histogram of **BTh4** in a semi-logarithmic scale. We observed peaks for the breaking of Au-Au contacts as marked by integers of G_0, and one well-defined molecular-junction related feature. A Gaussian fit led to $G^* = 10^{-4}$ G_0 as the most probable single molecular junction conductance of **BTh4**. This value appears to be independent of the concentration of **BTh4** down to 1 μM.

The above analysis was extended by constructing all-data point two-dimensional (2D) conductance vs. displacement histograms.[43,44] This representation provides direct access to the evolution of molecular junctions during the formation, stretching and break-down steps. Figure 2C shows the corresponding data for **BTh4**. The individual G - Δz traces were aligned by setting the common origin to Δz = 0 at G = 0.7 G_0. The data also reveal quantized conductance features at $G \geq 1$ G_0. They correspond to the breaking of gold-gold contacts. An additional high-density data cloud is observed in $10^{-4.5}$ $G_0 \leq G \leq 10^{-3.5}$ G_0, centred on 10^{-4} G_0. This region represents the conductance range of a single **BTh4** molecule bridging the gold nanoelectrodes. The 2D histogram in Figure 2C demonstrates further that the conductance decreases monotonously with increasing relative displacement (or junction

elongation) Δz. Similar results were obtained in complementary experiments employing the MCBJ-technique.

Analyzing the evolution of a molecular junction upon stretching we constructed relative displacement (Δz) histograms by calculating the displacement from the relative zero position at 0.7 G_0 up to the end of the molecular conductance region of every individual trace.[38] The lower limit is defined as one order of magnitude beneath the most probable conductance G_H. Figure 2D displays the characteristic displacement histograms of **BTh4**. The plot shows a uniform normal distribution (G) with a well-defined maximum Δz^* = (0.64 nm) as a measure of the most-probable plateau lengths of **BTh4** molecular junctions. Stretching traces shorter than 0.5 nm (T) were assigned to direct tunnelling through solution without the formation of a molecular junction.[38] This consideration leads to a junction formation probability of 30% (Table 2).

Finally, we obtain the most probable absolute displacements z_H^* in an experimental **BTh4** molecular junction formed between a gold STM-tip and an Au(111) surface by adding the snap-back distance Δz_{corr} = (0.5 ± 0.1) nm to the relative displacement Δz^*: $z_i^* = \Delta z^* + \Delta z_{corr}$,[38] which gives (1.14 ± 0.10) nm (Table 2). This value is smaller than the molecular length L, which is defined as the distance between the centre of the sulfur anchor atom at one end of a fully extended isolated molecule to the centre of the anchor atom at the other end. In other words, the molecular junctions formed with **BTh4** break most often before the molecule is completely extended.

Next, we investigated the entire family of tetrayne-type molecular junctions following the methodology described above for **BTh4**. Table 2 summarizes the characteristic data G^*, Δz^*, z^* and L for **BT4**, **PY4**, **CN4**, **$NO_2$4** and **BTh4**. The original traces can be found in the Supporting Information or in Ref. 31. We note that the low junction conductance value of **$NO_2$4** was obtained in the MCBJ set-up, which allows more sensitive electrical measurements down to $10^{-8.5}$ G_0.[39] We obtained the following trend in the most probable molecular junction conductances:

G^*(**BT4**) > G^*(**BTh4**) > G^*(**PY4**) > G^*(**CN**) > G^*(**$NO_2$4**)

The junction formation probabilities decrease from 100% for **BT4** and **PY4** to values below 50% for the other three derivatives. In combination with the values of the most probable absolute displacements z^*, which are considerably smaller than the molecular length L, we conclude that tetrayne-type molecular junctions terminated with **CN**-, **BTh**- and **NO_2**- anchors are rather unstable and break at an inclined angle with respect to the surface normal before they are fully extended. The comparison with previous experimental observations[31,38] suggests that these termini are less favourable for the formation of stable molecular junctions. However, we note that the results of the current study deviate from recent observations of Zotti *et al.*[45] who concluded, based on MCBJ

experiments in air under ambient conditions, that molecular junctions formed with **NO_2**-capped tolanes are rather stable. This difference may arise from the nature of the different experimental conditions in both studies.

We note that no reliable single molecule junction conductance measurements could be carried out for **NHMe4**, **$DMeNH_2$4**, **IN4**, **$NH_2$4** and **SH4** due to their limited chemical stability under current experimental conditions. In the case of **$NMe_2$4** the two methyl substituents of the nitrogen prevented the formation of stable molecular contacts, which led to bare tunneling traces.

Table 2. Single molecule conductance characteristics of molecular junctions formed by end-capped tetraynes attached to gold leads.

Molecule	L / nm[a]	Δz^*/ nm[b]	z^*/ nm[c]	G^*/G_0	JFP / %[d]	β / nm^{-1}[e]	R_c/ kΩ[f]
BT4	2.08	1.40 ± 0.10	1.90 ± 0.10	2.0×10^{-4}	100	3.1 ± 0.2	115 ± 31
PY4	1.76	1.40 ± 0.10	1.90 ± 0.10	4.0×10^{-5}	100	2.9 ± 0.2	1900 ± 1100
CN4	2.28	0.70 ± 0.10	1.20 ± 0.10	4.0×10^{-6}	45	1.75 ± 0.1	58000 ± 20100
$NO_2$4[g]	2.14	0.60 ± 0.10	1.10 ± 0.10	1.0×10^{-7}	40	5.4 ± 0.3	980 ± 500
BTh4	2.08	0.64 ± 0.10	1.14 ± 0.10	1.0×10^{-4}	30	2.3 ± 0.2	1050 ± 650

[a] molecular length L, which is defined as the distance between the centre of the anchor atom at one end of a fully extended isolated molecule to the centre of the anchor atom at the other end. The lengths of the molecules were obtained from crystal structure data. [b] Δz^* is the most probable relative junction elongation (displacement); [c] $z^* = \Delta z^* + 0.5$ is the absolute junction elongation (displacement), [d] JFP is the junction formation probability, [e] β is the attenuation parameter as obtained from the length dependence (L) of families of oligoynes with 4, 2 and 1 triple bond(s) end-capped with the respective anchors (some of the original data are taken from ref. [31]. [f] Contact resistance as obtained from the semi-logarithmic correlation of conductance G versus molecular length L. [g] These data are based on the analysis of 600 out of 2000 traces (for details see SI).

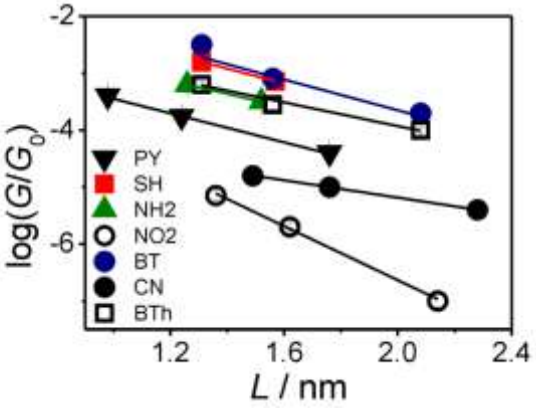

Figure 3. Most probable single junction conductance values G^* of families of oligoynes as obtained from the analysis of the 1D and 2D conductance histograms in dependence on the length of the molecule.

Next, we compare in Figure 3 the dependencies of the most probable single junction conductances on molecular length L, as constructed from the experimental data of the five tetraynes (**PY4**,[31] **$NO_2$4**,

BT4,[31] **CN4**[31] and **BTh4**) together with data for the shorter butadiyne and tolane analogues with seven different end-groups. Analyzing these data with reference to a simple tunnelling model, which is represented by $G^* = G^*_c \cdot \exp(-\beta \cdot L)$, leads to the attenuation constant β and to the contact conductance G_c^*. $G_c^* = 1/R_c$ represents an effective contact conductance reflecting the electronic coupling at the molecule-electrode interface. R_c is the corresponding contact resistance. β is the attenuation constant, which characterizes the electronic coupling in a specific molecular backbone as a function of its length. The experimentally determined β values range between (1.75 ± 0.1) nm^{-1} (CN) to (5.4 ± 0.3) nm^{-1} (NO_2). The distinctly different values of β demonstrate that the nature of the anchor group controls the strength of the electronic coupling to the metal leads, the position of the energy levels involved in the electron transport across the single molecule junction as well as their coupling into the wire backbone. For comparison, we also added the **NH_2** and **SH** end-capped oligoynes despite the limited data set due to the instability of the tetraynes.[31] The resulting values of the attenuation constant β are comparable with those of other π-conjugated molecular wires, such as oligo(phenylene-ethynylenes),[41,46,47,48,49,50] oligophenyleneimine[51] and oligo(phenylene-vinylenes).[46] We conclude that stable molecular wires bearing an oligoyne backbone in combination with proper anchoring groups may act as promising building blocks in more complex molecular assemblies combining functional units.

Conclusions

We have synthesized new oligoyne derivatives with emphasis on obtaining stable diaryltetraynes with anchor groups that are suitable for attaching the molecules to gold electrodes. The tetraynes **Ar4a-f** have been synthesised by dimerization of the trimethylsilyl-protected precursor aryldiyne derivative under classical Eglington-Galbraith coupling conditions. Under ambient laboratory conditions (20 ^oC, daylight and in air) the tetraynes **$NO_2$4** and **BTh4** are stable for at least six months without observable decomposition, whereas **NHMe4**, **$NMe_2$4**, **DMe$NH_2$4** and **IN4** decompose within a few hours or days. These results, in combination with previous studies,[31] provide a comprehensive assessment of the range of functional groups which can be tolerated at the terminal positions of diaryloligoynes. The X-ray molecular structures are reported for **$NO_2$4**, **NHMe4**, **DMe$NH_2$4**, **IN4** and **BTh4**. STM-BJ and MCBJ techniques have been employed to probe the single-molecule conductance characteristics of the series of oligoynes with terminal 4-nitrophenyl and 5-benzothienyl groups and four, two and one triple bond(s) in the backbone. We conclude that with careful choice of the anchor group oligoynes are a viable family of stable molecular wires for molecular electronics applications. It remains a challenge to synthesize longer oligoynes (i.e. with > four triple bonds) that are stable and contain functional groups that enable the molecules to anchor to gold electrodes.

Experimental Section

General: All reactions were conducted under a blanket of argon which was dried by passage through a column of phosphorus pentoxide unless otherwise stated. All commercial chemicals were used without further purification. Anhydrous toluene, tetrahydrofuran (THF), dichloromethane (DCM) and diethyl ether (Et_2O) were dried through an HPLC column on an Innovative Technology Inc. solvent purification system. Petroleum ether (PE) used for column chromatography is bp. 40-60 °C fractions and was used as received. Column chromatography was carried out using 40-60 μm mesh silica (Fluorochem). Analytical thin layer chromatography (TLC) was performed on 20 mm pre-coated plates of silica gel (Merck, silica gel 60F254); visualization was made using ultraviolet light (254 and 365 nm). NMR spectra were recorded on: Bruker Avance-400, Varian VNMRS 700 and Varian Inova 500 spectrometers. Chemical shifts are reported in ppm relative to $CDCl_3$ (7.26 ppm), acetone-d_6 (2.09 ppm), DMSO-d_6 (2.50 ppm) or tetramethylsilane (0.00 ppm). Melting points were determined in open-ended capillaries using a Stuart Scientific SMP40 melting point apparatus at a ramping rate of 2 °C/min. Mass spectra were measured on a Waters Xevo OTofMS with an ASAP probe. Electron ionisation (EI) mass spectra were recorded on a Thermoquest Trace or a Thermo-Finnigan DSQ. Ion analyses were performed on a Dionex 120 Ion Chromatography detector. Elemental analyses were performed on a CE-400 Elemental Analyzer. IR spectra were obtained on a Perkin Elmer FT-IR Paragon 1000 spectrometer. UV-Vis absorption spectra were obtained on a Unicam UV2 UV/Vis spectrometer. **CAUTION!** We did not attempt to measure the melting points of the diaryltetrayne derivatives, as on a previous occasion we observed that 1,8-bis(4-cyanophenyl)octa-1,3,5,7-tetrayne (CN4) exploded upon heating.[31]

General Procedure (I) for Sonogashira Couplings: The iodoarene derivative (1 eq), [$Pd(PPh_3)_4$] (5% mmol) and CuI (2% mmol) were placed in a dry flask and dissolved in THF (7 ml per mmol) and (i-Pr)$_2$NH or Et_3N (1 ml per mmol) to which the alkyne was added in small portions in 15 min. The mixture was stirred under argon at rt until the reaction was complete (judged by TLC). Solvents were removed and the crude was purified by column chromatography.

General Procedure (II) for Oxidative Homo-Couplings of TMS-Alkynes: TMS-alkyne was dissolved in MeOH/pyridine (1:1 v/v) mixture (10 ml per mmol) and $Cu(OAc)_2.H_2O$ (2 equiv., 0.400 g per mmol) was added to the mixture in one portion and stirred until the reaction is complete (judged by TLC). The reaction was quenched by adding saturated NH_4Cl solution (5 ml per mmol) and diluted with DCM (25 ml per mmol), dried over $MgSO_4$ and the solvents were removed under reduced pressure. The crude was purified either by column chromatography or recrystallization.

Compounds **1b**,[52] **1c**,[53] **1d**[54] BDTMS (**2**),[55] **3c**,[56] **4**[57] and **$NMe_2$4**[55] were synthesized according to the literature procedures. **1a** and **1e** were obtained commercially.

Trimethyl[(4-nitrophenyl)buta-1,3-diyn-1-yl]silane (3a). *General Procedure (I)*: 4-iodonitrobenzene (**1a**) (0.400g, 1.6 mmol), BDTMS (**2)** (0.216 g, 1.77 mmol), [$Pd(PPh_3)_4$] (92 mg), CuI (6 mg), (*i*-Pr)$_2$NH, overnight, rt. Purified by column chromatography using DCM/hexane (1:1, v/v) as eluent to afford **3a** as a yellow solid (0.30 g, 77% yield). mp: 110.0 - 111.0 °C. ^{1}H NMR (400 MHz, $CDCl_3$) δ 8.18 (d, *J* = 9.0 Hz, 2H), 7.61 (d, *J* = 9.0 Hz, 2H), 0.24 (s, 9H). ^{13}C NMR (101 MHz, $CDCl_3$) δ 147.75, 133.62, 128.58, 123.87, 94.45, 87.12, 79.19, 74.37, -0.32. MS (ES^+) *m/z* (%): 244.0 ($[M+H]^+$, 100). The data are consistent with the literature.[58]

1,8-Bis(4-nitrophenyl)octa-1,3,5,7-tetrayne ($NO_2$4). *General procedure (II)*: **3a** (0.200 g, 0.82 mmol) and $Cu(OAc)_2.H_2O$ (0.328 g, 1.64 mmol). The mixture was stirred for 12 h at rt. The yellow-green precipitate was filtered and recrystallized from toluene to give **$NO_2$4** as air-stable yellow crystals (0.12 g, 43% yield). Reliable NMR spectra could not be obtained due to the compound's very low solubility in standard NMR solvents, including C_6D_6 which is stated in reference 33 as the NMR solvent for this compound. MS (ES) *m/z*: 341.1 [M^++H]. HR-MS ($ASAP^+$) *m/z* calcd for $C_{20}H_8N_2O_4$ 340.0484, found 340.0466 [M^+]. IR (solid) ν 3106, 2202, 1589, 1516, 1340, 1287, 1103, 1014, 851, 745, 682 cm^{-1}. UV/Vis (CH_2Cl_2) λ_{max} (ε) 317 (84600), 334 (96000), 356 (85200), 384 (72400), 416 (44800 M^{-1} cm^{-1}) nm. Crystals for X-ray analysis were grown by slow evaporation of a solution in toluene. CCDC number 938775.

***N*-Methyl-4-[(trimethylsilyl)buta-1,3-diyn-1-yl]aniline (3b)**. *General procedure (I)*: **1b** (0.500 g, 2.1 mmol), BDTMS (**2**) (0.525, 4.20 mmol), [$Pd(PPh_3)_4$] (0.124g) and CuI (10 mg) stirred at rt for 4 h. Column chromatography (DCM/PE, 1:1 v/v) gave **3b** as yellow, light sensitive oil (0.445 g, 95% yield). ^{1}H NMR (400 MHz, $CDCl_3$) δ 7.31 (d, *J* = 8.8 Hz, 2H), 6.48 (d, *J* = 8.8 Hz, 2H), 4.01 (s, 1H), 2.83 (s, 3H), 0.22 (s, 9H). ^{13}C NMR (101 MHz, $CDCl_3$) δ 150.24, 134.44, 112.11, 108.54, 89.56, 88.89, 78.86, 72.49, 30.45, -0.01. MS (ES) *m/z* : 228.2 [M^++H, 100%].

4,4'-(Octa-1,3,5,7-tetrayne-1,8-diyl)bis(*N*-methylaniline) (NHMe4). *General procedure (II)*: Compound **3b** (0.200 g, 0.88 mmol), $Cu(OAc)_2.H_2O$ (0.351g). The mixture was stirred for 16 h at rt. Column chromatography (DCM/PE, 1/1 v/v) to gave **NHMe4** as a yellow solid (0.111 g, 81% yield). ^{1}H NMR (400 MHz, $CDCl_3$) δ 7.36 (d, *J* = 8.4 Hz, 4H), 6.49 (d, *J* = 8.4 Hz, 4H), 4.07 (s, 2H), 2.86 (s, 6H). ^{13}C NMR (101 MHz, $CDCl_3$) δ 150.56, 135.11, 112.15, 107.76, 79.79, 73.39, 67.53, 64.67, 30.39. HR-MS ($ASAP^+$) *m/z* calcd for $C_{22}H_{17}N_2$ [M^++H]. 309.1371, found 309.1414 [M^++H]. Crystals for X-ray analysis were grown by slow evaporation of a solution in $CHCl_3$. CCDC number 938776.

3,5-Dimethyl-4-[(trimethylsilyl)buta-1,3-diyn-1-yl]aniline (3d). *General Procedure (I)*: **1d**[59] (0.300 g, 1.21 mmol), BDTMS (**2**) (0.297g, 2.43 mmol), [$Pd(PPh_3)_4$] (70 mg), (i-Pr)$_2$NH, CuI (5 mg), 20 min, microwave reactor, 100 °C. Purified by column chromatography using DCM/PE (1:1, v/v) as eluent to afford **3d** as a brownish oil (40 mg, 13%). ^{1}H NMR (400 MHz, $CDCl_3$) δ 6.32 (s, 2H), 3.76 (s, 2H), 2.34 (s, 6H), 0.23 (s, 9H). ^{13}C NMR (101 MHz, $CDCl_3$) δ 147.17, 144.37, 113.52, 110.84, 90.50, 88.92, 80.05, 76.21, 21.32, 0.03. MS (ES^+) *m/z* : 241.1 ($[M]^+$, 40).

4,4'-(Octa-1,3,5,7-tetrayne-1,8-diyl)bis(3,5-dimethylaniline) (DMeNH$_2$4). *General Procedure (II)*: **3d** (40 mg, 0.16 mmol), $Cu(OAc)_2.H_2O$ (66 mg), overnight, rt. Purified by column chromatography using DCM as eluent to afford **DMeNH$_2$4** as a yellow solid (18 mg, 65%). ^{1}H NMR (400 MHz, Acetone-d_6) δ 6.41 (s, 4H), 5.27 (s, 4H), 2.29 (s, 12H). ^{13}C NMR (101 MHz, $CDCl_3$) δ 155.72, 150.04, 118.21, 111.92, 84.91, 84.36, 73.54, 70.66, 25.66. HR-MS ($ASAP^+$) m/z calcd for $C_{24}H_{21}N_2$ $[M+H]^+$ 337.1699, found *m/z* : $[M+H]^+$ 337.1711. UV/Vis (CH_2Cl_2) λ_{max} (ε) 306 (54527), 325 (78844), 360 (94907), 378 (96986), 411 (63976 M^{-1} cm^{-1}) nm. Crystals for X-ray analysis were grown by slow evaporation of of a solution in acetone in the dark. CCDC number 938777.

1,8-Bis(indol-5-yl)octa-1,3,5,7-tetrayne (IN4). *General Procedure (I):* 5-iodoindole **(1e)** (300 mg, 1.23 mmol), CuI (12 mg), [$Pd(PPh_3)_4$] (70 mg), BDTMS (**2**) (226 mg, 1.85 mmol), THF/Et_3N (10 ml), 24 h, 50 °C. The solvent was removed by vacuum evaporation to yield a product which could not be purified by column chromatography. *General Procedure (II)* was conducted directly on the brown crude material: $Cu(OAc)_2.H_2O$ (320 mg), MeOH/pyridine (4 ml/4 ml) 23 h, rt. Purification by column chromatography using DCM/hexane (3:7 v/v) as eluent gave a yellow solid (70 mg, 35% overall yield), mp: 130 °C (dec.) which turned green in ambient conditions within a week. ^{1}H NMR (400 MHz, (DMSO-d_6) δ 11.51 (s, 2H), 7.94 (s, 2H), 7.47 (m, 2H), 7.43 (d, J = 8.4 Hz, 2H), 7.32 (dd, J = 8.4, 1.6 Hz, 2H), 6.49 (m, 2H). ^{13}C NMR (101 MHz, DMSO-d_6) δ 137.46, 128.33, 128.25, 127.57, 126.39, 113.10, 109.12, 102.51, 82.29, 72.35, 66.93, 65.04. HR-MS ($ASAP^+$) *m/z* Calcd for $C_{24}H_{12}N_2$ $[M]^+$ 328.1000, found m/z : $[M]^+$ 328.1014. Crystals for X-ray analysis were grown by slow evaporation of a solution in dichloromethane/hexane in the dark. CCDC number 973876.

[(Benzothiophen-5-yl)buta-1,3-diyn-1-yl]trimethylsilane (3f). Trimethylsilylacetylene (TMSA) (930 mg, 9.4 mmol), [$Pd(PPh_3)Cl_2$] (33 mg) and CuI (9 mg) was added to a solution of **4** (150 mg, 0.94 mmol) in THF/Et_3N (9 ml / 3 ml). Air was bubbled constantly through the solution until the reaction was complete after 12 hours at rt. Purification by column chromatography using PE as eluent gave **3f** as a yellow solid (90 mg, 38% yield). mp: 91.3-92.4 °C. ^{1}H NMR (400 MHz, $CDCl_3$) δ 7.97 (s, 1H), 7.81 (d, J = 8.3 Hz, 1H), 7.48 (d, J = 5.5 Hz, 1H), 7.44 (d, J = 8.3 Hz, 1H), 7.30 (d, J = 5.5 Hz, 1H), 0.26 (s, 9H). ^{13}C NMR (101 MHz, $CDCl_3$) δ 140.93, 139.66, 128.47, 128.06, 127.96, 123.87,

122.84, 117.36, 90.67, 88.24, 77.46, 73.98, 0.00. HR-MS (ASAP$^+$) *m/z* Calcd for $C_{15}H_{15}SiS$ $[M+H]^+$ 255.0664, found *m/z* : $[M+H]^+$ 255.0662.

1,8-Bis(benzothiophen-5-yl)octa-1,3,5,7-tetrayne (BTh4). *General Procedure (II)*: **3f** (80 mg, 0.31 mmol), $Cu(OAc)_2.H_2O$ (130 mg), MeOH/pyridine (3 ml/3 ml), 22 h, rt. Purification by column chromatography using DCM/PE (5:95 v/v) as eluent gave **BTh4** as a bright yellow solid (50 mg, 87% yield). mp: 160 ^oC (decomp.). ^1H NMR (600 MHz, CD_2Cl_2) δ 8.08 (s, 2H), 7.89 (d, *J* = 8.3 Hz, 2H), 7.57 (d, *J* = 5.5 Hz, 2H), 7.51 (d, *J* = 8.3 Hz, 2H), 7.38 (d, *J* = 5.5 Hz, 2H). ^{13}C NMR (151 MHz, CD_2Cl_2) δ 141.54, 139.53, 128.92, 128.18, 127.97, 123.59, 122.82, 115.95, 78.38, 73.60, 66.73, 63.63. HR-MS (ASAP$^+$) *m/z* Calcd for $C_{24}H_{10}S_2$ $[M]^+$ 362.0224, found *m/z* : $[M]^+$ 362.0224. IR (solid) ν 2192, 1897, 1591, 1435, 1326, 1253, 1168, 1087, 1050, 1002, 883, 867, 805, 744, 683 cm^{-1}. UV/Vis (CH_2Cl_2) λ_{max} (ε) 309 (130301), 328 (136920), 350 (69825), 377 (69282), 409 (43824 M^{-1} cm^{-1}) nm. Crystals for X-ray analysis were grown by by slow evaporation of a solution in dichloromethane/acetone. CCDC number 938778.

Conductance Measurements. The STM-BJ experiments were carried out with a modified Molecular Imaging Pico SPM equipped with a dual-channel preamplifier and housed in an all-glass argon-filled chamber.[38] The current (i_T) - distance (Δz) measurements were performed with a separate, lab-built analog ramp unit. The sample electrodes were Au(111) disks, 2 mm height and 10 mm in diameter, or gold single crystal bead electrodes. The Au(111) substrates were flame-annealed before each experiment. The STM tips were uncoated, electrochemically etched gold wires (Goodfellow, 99.999%, 0.25 mm diameter). The solutions were prepared from 1,3,5-trimethylbenzene (TMB, Aldrich, p.a.) and tetrahydrofuran (THF, Aldrich, p.a.), volume ratio 4 : 1, containing typically 0.1 mM of the target molecules. The substrate surface was inspected by STM-imaging before the start of each set of i_T - Δz measurements. Typically, we recorded 2000 to 3000 individual traces with a pulling rate of 58 nm s^{-1}.

The MCBJ experiments are based on the trapping of individual molecules between two atomically sharp gold wires (99.999%, Goodfellow, 100 μm diameter), freely suspended and supported on a sheet of spring steel. The latter is bent by a pushing rod, whose vertical movement is controlled by a stepper motor in combination with a piezo stack. The usual moving rate of the pushing rod was 3 to 150 nm s^{-1}, which translates into an opening respective closing rate of 0.1 to 5 nm s^{-1}. Typically, we recorded up to 2000 stretching cycles to obtain statistically significant data.

Supporting Information: Supporting information for this article is available on the WWW under http://dx.doi.org/xxxx

Acknowledgements: The work was funded by the EC FP7 ITNs "FUNMOLS" Project No. 212942 and "MOLESCO" Project No. 606728, the Swiss National Science Foundation under contract 200020_144471/1 and the University of Bern. Z. X. thanks the China Scholarship Council for the award of a scholarship.

[1] M. M. Haley, R. R. Tykwinski (Eds.), *Carbon-Rich Compounds* : *From Molecules to Materials*, Wiley-VCH, Weinheim, **2006**.

[2] F. Diederich, P. J. Stang, R. R. Tykwinski (Eds.), *Acetylene Chemistry: Chemistry, Biology and Material Science*; Wiley-VCH, Weinheim, **2005**.

[3] a) D. M. Guldi, N. Martin, M. Prato (Eds.), *J. Mater. Chem.* Theme Issue: Carbon Nanostructures, **2008**, *18*, 1401–1604; b) D. M. Guldi, B. M. Illescas, C. M. Atienza, M. Wielopolski, N. Martin, *Chem. Soc. Rev*. **2009**, 38, 1587–1597; c) L. Rodriguez-Perez, M. A. Herranz, N. Martin, *Chem. Commun*. **2013**, *49*, 3721–3735.

[4] a) F. Diederich, *Nature* **1994**, *369*, 199–207; b) W. A. Chalifoux, R. R. Tykwinski, *C. R. Chim*. **2009**, *12*, 341–358.

[5] F. Cataldo (Ed.), *Polyynes: Synthesis Properties and Applications*, CRC Press, Taylor & Francis Group, Boca Raton, FL, **2006**.

[6] E. Jahnke, R. R. Tykwinski, *Chem. Commun*. **2010**, *46*, 3235–3249.

[7] S. A. Vail, P. J. Krawczuk, D. M. Guldi, A. Palkar, L. Echegoyen, J. P. C. Tome, J. M. A. Fazio, D. I. Schuster, *Chem.- Eur. J.* **2005**, *11*, 3375–3388.

[8] C. Wang, L.-O. Palsson, A. S. Batsanov, M. R. Bryce, *J. Am. Chem. Soc*. **2006**, *128*, 3789–3799.

[9] L.-O. Pålsson, C. Wang, A. S. Batsanov, S. M. King, A. Beeby, A. P. Monkman, M. R. Bryce, *Chem. Eur. J*. **2010**, *16*, 1470–1479.

[10] F. Cataldo, L. Ravagnan, E. Cinquanta, I. E. Castelli, N. Manini, G. Onida, P. Milani, *J. Phys. Chem. B* **2010**, *114*, 14834–14841.

[11] P. O. Dral, T. Clark, *J. Phys. Chem. A* **2011**, *115*, 11303–11312.

[12] J. Cornil, D. Beljonne, J. P. Calbert, J. L. Brédas, *Adv. Mater.* **2001**, *13*, 1053–1067.

[13] A. D. Slepkov, F. A. Hegmann, S. Eisler, E. Elliott, R. R. Tykwinski, *J. Chem. Phys.* **2004**, *120*, 6807–6810.

[14] Z. Crljen, G. Baranović, *Phys. Rev. Lett.* **2007**, *98*, 116801.

[15] V. M. Garcia-Suarez, C. J. Lambert, *Nanotechnology* **2008**, *19*, 455203.

[16] R. Eastmond, T. R. Johnson, D. R. M. Walton, *Tetrahedron* **1972**, *28*, 4601–4616.

[17] a) J. Kendall, R. McDonald, M. J. Ferguson, R. R. Tykwinski, *Org. Lett.* **2008**, *10*, 2163–2166; b) Y. Rubin, S. S. Lin, C. B. Knobler, J. Anthony, A. M. Boldi, F. Diederich, *J. Am. Chem. Soc*. **1991**, *113*, 6943–6949.

[18] T. Gibtner, F. Hampel, J.-P. Gisselbrecht, A. Hirsch, *Chem. Eur. J.* **2002**, *8*, 408–432.

[19] T. Luu, E. Elliott, A. D. Slepkov, S. Eisler, R. McDonald, F. A. Hegmann, R. R. Tykwinski, *Org. Lett.* **2004**, *7*, 51–54.

[20] a) W. Mohr, J. Stahl, F. Hampel, J. A. Gladysz, *Chem. Eur. J.* **2003**, *9*, 3324–334; b) S. Szafert, J. A. Gladysz, *Chem. Rev.* **2003**, *103*, 4175–4206.

[21] C. Wang, A. S. Batsanov, K. West, M. R. Bryce, *Org. Lett.* **2008**, *10*, 3069–3072.

[22] C. Klinger, O. Vostrowsky, A. Hirsch, A. *Eur. J. Org. Chem.* **2006**, 1508–1524.

[23] J. Sugiyama, I. Tomita, I. *Eur. J. Org. Chem.* **2007**, 4651–4653.

[24] L. D. Movsisyan, D. V. Kondratuk, M. Franz, A. L. Thompson, R. R. Tykwinski, H. L. Anderson, *Org. Lett*. **2013**, *14*, 3424–3426.

[25] N. Weisbach, Z. Baranova, S. Gauthier, J. H. Reibenspies, J. A. Gladysz, *Chem. Commun*. **2012**, *48*, 7562–7564.

[26] C. Zhao, R. Kitaura, H. Hara, S. Irle, H. Shinohara, *J. Phys. Chem. C* **2011**, *115*, 13166–13170.

[27] W. A. Chalifoux, R. R. Tykwinski, *Nat. Chem.* **2010**, *2*, 967–971.

[28] N. Weibel, S. Grunder, M. Mayor, *Org. Biomol. Chem.* **2007**, *5*, 2343–2353.

[29] R. Ziessel, J. Suffert, M.-T. Youinou, *J. Org. Chem.* **1996**, *61*, 6535–6546.

[30] C. Wang, A. S. Batsanov, M. R. Bryce, S. Martin, R. J. Nichols, S. J. Higgins, V. M. Garcia-Suarez, C. J. Lambert, *J. Am. Chem. Soc.* **2009**, *131*, 15647–15654.

[31] P. Moreno-García, M. Gulcur, D. Z. Manrique, T. Pope, W. Hong, V. Kaliginedi, C. Huang, A. S. Batsanov, M. R. Bryce, C. Lambert, T. Wandlowski, *J. Am. Chem. Soc*. **2013**, *135*, 12228–12240.

[32] G. Eglington, A. R. Galbraith, *J. Chem. Soc*. **1958**, 889–896.

[33] N. Gulia, K. Osowska, B. Pigulski, T. Lis, Z. Galewski, S. Szafert, *Eur. J. Org. Chem*. **2012**, 4819–4830.

[34] M. Stefko, M. D. Tzirakis, B. Breiten, M.-O. Ebert, O. Dumele, W. B. Schweizer, J.-P. Gisselbrecht, C. Boudon, M. T. Beels, I. Biaggio, F. Diederich, *Chem. Eur. J*. **2013**, *19*, 12693–12704.

[35] C. Li, I. Pobelov, T. Wandlowski, A. Bagrets, A. Arnold, F. Evers, *J. Am. Chem. Soc.* **2008**, *130*, 318–326.

[36] B. Q. Xu, N. J. Tao, *Science* **2003**, *301*, 1221–1223.

[37] R. Huber, M. T. Gonzalez, S. Wu, M. Langer, S. Grunder, V. Horhoiu, M. Mayor, M. R.

Bryce, C. S. Wang, R. Jitchati, C. Schonenberger, M. Calame, *J. Am. Chem. Soc.* **2008**, *130*, 1080–1084.

[38] W. Hong, D. Z. Manrique, P. Moreno-García, M. Gulcur, A. Mishchenko, C. J. Lambert, M. R. Bryce, T. Wandlowski, *J. Am. Chem. Soc.* **2012**, *134*, 2292–2304.

[39] W. Hong, H. Valkenier, G. Mészáros, D. Z. Manrique, A. Mishchenko, A. Putz, P. M. García, C. J. Lambert, J. C. Hummelen, T. Wandlowski, *Beilstein J. Nanotechnol.* **2011**, *2*, 699–713.

[40] G. Meszaros, C. Li, I. Pobelov, T. Wandlowski, *Nanotechnology* **2007**, *18*, 424004.

[41] V. Kaliginedi, P. Moreno-García, H. Valkenier, W. Hong, V. M. García-Suárez, P. Buiter, J. L. H. Otten, J. C. Hummelen, C. J. Lambert, T. Wandlowski, *J. Am. Chem. Soc.* **2012**, *134*, 5262–5275.

[42] S. Y. Quek, M. Kamenetska, M. L. Steigerwald, H. J. Choi, S. G. Louie, M. S. Hybertsen, J. B. Neaton, L. Venkataraman, *Nat. Nanotechnol.* **2009**, *4*, 230–234.

[43] A. Mishchenko, L. A. Zotti, D. Vonlanthen, M. Burkle, F. Pauly, J. C. Cuevas, M. Mayor, T. Wandlowski, *J. Am. Chem. Soc.* **2011**, *133*, 184–187.

[44] C. A. Martin, D. Ding, J. K. Sorensen, T. Bjornholm, J. M. van Ruitenbeek, H. S. J. van der Zant, *J. Am. Chem. Soc.* **2008**, *130*, 13198–13199.

[45] L. A. Zotti, T. Kirchner, J. C. Cuevas, F. Pauly, T. Huhn, E. Scheer, A. Erbe, *Small* **2010**, *6*, 1529–1535.

[46] H. M. Liu, N. Wang, J. W. Zhao, Y. Guo, X. Yin, F. Y. C. Boey, H. Zhang, *ChemPhysChem.* **2008**, *9*, 1416–1424.

[47] Y. J. Xing, T. H. Park, R. Venkatramani, S. Keinan, D. N. Beratan, M. J. Therien, E. Borguet, *J. Am. Chem. Soc.* **2010**, *132*, 7946–7956.

[48] Q. Lu, K. Liu, H. M. Zhang, Z. B. Du, X. H. Wang, F. S. Wang, *ACS Nano* **2009**, *3*, 3861–3868.

[49] K. Liu, G. Li, X. Wang, F Wang, *J. Phys. Chem. C* **2008**, *112*, 4342–4349.

[50] X. Zhao, C. Huang, M. Gulcur, A. S. Batsanov, M. Baghernejad, W. Hong, M. R. Bryce, T. Wandlowski, *Chem. Mater.* **2013**, *25*, 4340–4347.

[51] S. H. Choi, B. Kim, C. D. Frisbie, *Science* **2008**, *320*, 1482–1486.

[52] W. Qu, M.-P. Kung, C. Hou, S. Oya, H. F. Kung, *J. Med. Chem.* **2007**, *50*, 3380–3387.

[53] K. A. Leonard, M. I. Nelen, L. T. Anderson, S. L. Gibson, R. Hilf, M. R. Detty, *J. Med. Chem.* **1999**, *42*, 3942–3952.

[54] S. Kajigaeshi, T. Kakinami, H. Yamasaki, S. Fujisaki, T. Okamoto, *Bull. Chem. Soc. Jap.* **1988**, *61*, 600–602.

[55] M. I. Bruce, P. J. Low, A. Werth, B. W. Skelton, A. H. White, *J. Chem. Soc., Dalton Trans.* **1996**, 1551–1566.

[56] M. Kivala, C. Boudon, J. P. Gisselbrecht, P. Seiler, M. Gross, F. Diederich, *Angew. Chem. Int. Ed.* **2007**, *46*, 6357–6360.

[57] P. A. Wender, A. B. Lesser, L. E. Sirois, *Angew. Chem. Int. Ed.* **2012**, *51*, 2736–2740.

[58] S. G. Kwon, Y. Piao, J. Park, S. Angappane, Y. Jo, N.-M. Hwang, J.-G. Park, T. Hyeon, *J. Am. Chem. Soc.* **2007**, *129*, 12571–12584.